JACS
JOURNAL OF THE AMERICAN CHEMICAL SOCIETY
Article
pubs.acs.org/JACS

A Complete High-to-Low spin state Transition of Trivalent Cobalt Ion in Octahedral Symmetry in $SrCo_{0.5}Ru_{0.5}O_{3-\delta}$

Jin-Ming Chen,[†] Yi-Ying Chin,[†,‡] Martin Valldor,*[,‡,§] Zhiwei Hu,[‡] Jenn-Min Lee,[†] Shu-Chih Haw,[†] Nozomu Hiraoka,[†] Hirofumi Ishii,[†] Chih-Wen Pao,[†] Ku-Ding Tsuei,[†] Jyh-Fu Lee,[†] Hong-Ji Lin,[†] Ling-Yun Jang,[†] Arata Tanaka,[∥] Chien-Te Chen,[†] and Liu Hao Tjeng[‡]

[†]National Synchrotron Radiation Research Center, 101 Hsin Ann Road, Hsinchu 30076, Taiwan, R.O.C.
[‡]Max Planck Institute for Chemical Physics of Solids, Nöthnitzer Strasse 40, 01187 Dresden, Germany
[§]II. Physikalisches Institut, Universität zu Köln, Zuelpicher Strasse 77, D-50937 Köln, Germany
[∥]Department of Quantum Matter, ADSM, Hiroshima University, 1-3-1 Kagamiyama, Higashi - Hiroshima 739-8530, Japan

Supporting Information

ABSTRACT: The complex metal oxide $SrCo_{0.5}Ru_{0.5}O_{3-\delta}$ possesses a slightly distorted perovskite crystal structure. Its insulating nature infers a well-defined charge distribution, and the six-fold coordinated transition metals have the oxidation states +5 for ruthenium and +3 for cobalt as observed by X-ray spectroscopy. We have discovered that Co^{3+} ion is purely high-spin at room temperature, which is unique for a Co^{3+} in an octahedral oxygen surrounding. We attribute this to the crystal field interaction being weaker than the Hund's-rule exchange due to a relatively large mean Co−O distances of 1.98(2) Å, as obtained by EXAFS and X-ray diffraction experiments. A gradual high-to-low spin state transition is completed by applying high hydrostatic pressure of up to 40 GPa. Across this spin state transition, the Co Kβ emission spectra can be fully explained by a weighted sum of the high-spin and low-spin spectra. Thereby is the much debated intermediate spin state of Co^{3+} absent in this material. These results allow us to draw an energy diagram depicting relative stabilities of the high-, intermediate-, and low-spin states as functions of the metal−oxygen bond length for a Co^{3+} ion in an octahedral coordination.

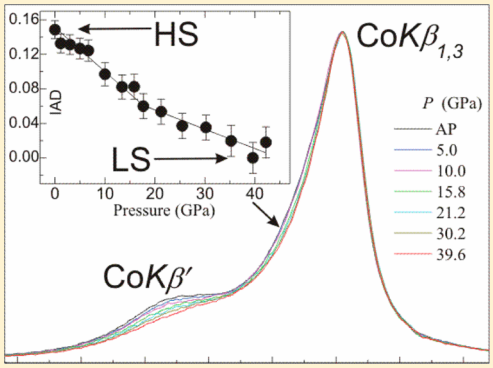

1. INTRODUCTION

Among the 3*d* transition metal ions, cobalt is outstanding because of its spin state degree of freedom. Apart from the high-spin (HS) and low-spin (LS) states, an intermediate spin state (IS) is also proposed in many cobalt compounds. The spin state of cobalt is affected by its formal oxidation state, the surrounding crystal field, the coordination number together with the local symmetry, and the type of neighboring ions. The spin degree of freedom of cobalt reflects the subtle balance between crystal field and Hund's rule exchange interaction. Hence, by properly choosing the external parameters, such as temperature and pressure, spin state instabilities can be achieved. Examples of the temperature-induced spin state crossover complexes are well-known in bis-(2,6-pyridindialdihydrazone)CoI_2[1] and $[PhB(CH_2PPh_2)_3]CoX$ (Ph = phenyl, X = I, Br, Cl).[2] Krivokapic et al. have gathered even more examples in their review.[3] The parameter pressure also can be used to induce a spin state transition of cobalt as in $K_{0.12}Co[Fe(CN)_6]_{0.70}\cdot 4.87H_2O$[4] and in $Co[C_{10}H_6N_5O_2]_2$.[5,6] The latter is also reported to transform from a high-spin Co^{2+} to a low-spin Co^{3+} through electrochemical treatment.[5] Naturally, in the spin crossover compounds high pressures and low temperatures favor a LS state.

The largest spin state variability of Co^{3+} is reported mainly for metal oxide compound, often within crystal structures where cobalt is coordinated by four to six oxygen ions. LS Co^{3+} is found in $LiCoO_2$,[7] $La_2Li_{0.5}Co_{0.5}O_4$,[8] and in $LaCoO_3$ at low temperature. The last is intensively studied and its controversial spin state crossover upon heating is still debated.[9,10] Co^{4+} was observed with all three spin states: LS in $BaCoO_3$,[11] IS Co^{4+} in Sr_2CoO_4[12] and $SrCoO_3$,[13] and HS in Ba_2CoO_4.[14] HS Co^{3+} in a tetrahedral local symmetry was found in a mixed valent cobalt oxide $YBaCo_4O_7$.[15] The pure HS Co^{3+} in a square pyramidal CoO_5 coordination occurs in Sr_2CoO_3Cl[16] and $BiCoO_3$.[17] The latter exhibits the HS to LS(IS) transition under high pressure,[18,19] accompanied by a CoO_5 to a CoO_6 coordination transition. However, the pure HS Co^{3+} oxide in octahedral local symmetry is rarely documented. Also, there is a steady debate on the issue whether the octahedrally coordinated Co^{3+} has a mixed HS−LS state or an IS state in the new classes of cobaltates $RBaCo_2O_{5.5}$ (R = rare-earth metal),[20] $Sr_{1-x}Y_xCoO_{3-\delta}$,[21] $Pr_{0.5}Ca_{0.5}CoO_3$,[22] as well as in $LaCoO_3$ at high temperature.[10,23,24]

Received: November 8, 2013
Published: January 10, 2014

   dx.doi.org/10.1021/ja4114006 | J. Am. Chem. Soc. 2014, 136, 1514−1519

$SrCo_{0.5}Ru_{0.5}O_{3-\delta}$ was first synthesized by Kim and Battle[25] and formally can be seen as a 1:1 solid solution of $SrRuO_3$ and $SrCoO_3$. Both parent compounds are metallic ferromagnets, but $SrCo_{0.5}Ru_{0.5}O_{3-\delta}$ exhibits spin-glass-like and semiconducting behaviors i.e. ~3 Ωcm at 300 K and ~3 × 10^3 Ωcm at 100 K.[25,26] The total effective magnetic moment of 4.9 μ_B per formula unit was obtained from high temperature magnetic susceptibility data but the transition metal oxidation states were discussed as either Co^{3+}/Ru^{5+} or Co^{4+}/Ru^{4+}.[26] Thus, $SrCo_{0.5}Ru_{0.5}O_{3-\delta}$ seems to be a good candidate for a spin state instability and enables us to explore three possible spin states within one compound. The chosen method is X-ray absorption spectroscopy (XAS) and X-ray emission spectroscopy to explore the oxidation state and spin state of cobalt along with the spin state transition upon applying high hydrostatic pressure.

In a broad view, all the extraordinary material properties of the cobaltates, including superconductivity,[27] giant magnetoresistance,[28] strong thermopower,[29] metal−insulator transitions,[17,22] as well as spin-blockade behavior[30,31] are related to the spin state degree of freedom of the cobalt ion. Hence, if the debate around the IS state is settled, the interpretations of the material properties of cobalt-based metal oxides are simplified remarkably.

2. EXPERIMENTAL SECTION

Synthesis and Basic Characterization. A powder $SrCo_{0.5}Ru_{0.5}O_{3-\delta}$ sample was prepared by solid-state reaction as described elsewhere.[25,26] A pellet of X-ray pure material was subsequently heated overnight in 9.5 bar of pure oxygen at 900 °C followed by 10 h slow cooling to room temperature. The oxygen content in our $SrCo_{0.5}Ru_{0.5}O_{3-\delta}$ sample was found to be 2.96 as determined by thermogravimetric hydrogen reduction (S1 in Supporting Information [SI]). The oxidized material proved to be pure by X-ray diffraction measurements, and the subsequent Rietveld refinement confirmed the crystal structure[25] with satisfying *R*-values (S2 in SI).

X-ray spectroscopy experiments. The Co-$L_{2,3}$ and Ru-$L_{2,3}$ XAS spectra were measured at beamlines BL11A and BL16A, respectively, of the National Synchrotron Radiation Research Center (NSRRC) in Taiwan. The pellet sample was fractured in situ in an ultrahigh-vacuum chamber with a pressure in the 10^{-10} mbar range. High-pressure Ru-*K* XAS and Co-*K* extended X-ray absorption fine structure (EXAFS) spectra were collected in the transmission geometry at beamlines BL07A and BL01C, respectively, of the NSRRC. The high pressure Co Kβ X-ray emission spectra were obtained at the Taiwan inelastic X-ray scattering BL12XU beamline at SPring-8 in Japan with an overall resolution of ~0.9 eV.

3. RESULTS AND DISCUSSIONS

The cobalt-to-oxygen distance. A detailed crystal structure description can be found elsewhere.[25] However, the average local surrounding of Co is important to understand the data presented below. Hence, Figure 1 displays the unit cell of the body centered monoclinic crystal structure as well as the local oxygen coordination of the transition metal site. From the crystal structure refinement (S2), it is obvious that the Co−O distances are unusually large, ranging from 1.96 to 2.00 Å (Figure 1).

As ruthenium and cobalt share one crystallographic site and the diffraction experiment gives an average picture, an elemental specific local probe was applied to confirm the Co−O distances, because of the great importance of the crystal field interaction on the transition metals spin state. The Co-*K* EXAFS data, shown in Figure 2A, were analyzed using the

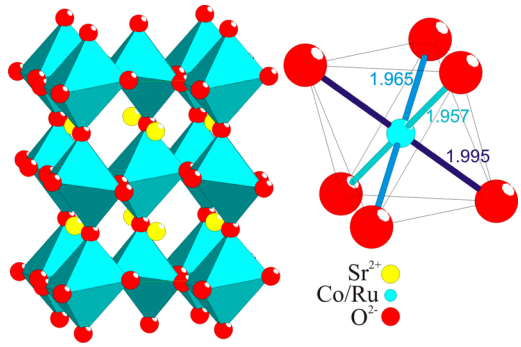

Figure 1. Part of the $SrCo_{0.5}Ru_{0.5}O_{2.96}$ crystal structure (left) and the local transition metal surrounding with bond lengths in Å to the neighboring oxygen ions (right).

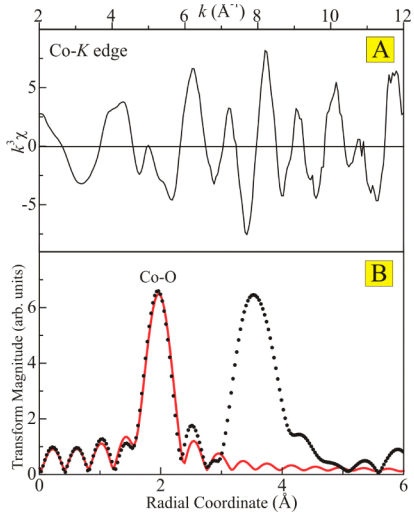

Figure 2. (A) Co-*K* EXAFS oscillations of $SrCo_{0.5}Ru_{0.5}O_{2.96}$ at ambient pressure and room temperature. (B) Experimental (filled circles) and simulated (full line) Fourier transforms of the k^3-weighted Co-*K* EXAFS spectrum.

IFEFFIT program. The results reveal an average Co−O distance of 1.98 ± 0.02 Å (Figure 2B). This distance agrees with those from the structural analysis and is even larger than that in $LaCoO_3$ at 1000 K.[32] At 650 K the average distance in $LaCoO_3$ was found to be 1.949 Å, a state which was proposed to have half of the cobalt ions in a HS state,[9] whereas Co−O distance for IS Co^{4+} ion in $SrCoO_3$ is 1.918 Å.[13]

Oxidation states of both transition metals. Although a Co^{3+}/Ru^{5+} charge distribution is more reasonable than Co^{4+}/Ru^{4+} considering the redox potentials, it is important to investigate the oxidation states of both transition metals in the title compound. In Figure 3, the Ru-$L_{2,3}$ XAS data are shown for $SrCo_{0.5}Ru_{0.5}O_{2.96}$ together with those of $Sr_4Ru_2O_9$[33] and $SrRuO_3$ as reference for Ru^{5+} and Ru^{4+} compounds, respectively. The figure reveals clearly that the Ru-$L_{2,3}$ spectrum of $SrCo_{0.5}Ru_{0.5}O_{2.96}$ has the same line shape as that of $Sr_4Ru_2O_9$ and differs from that of $SrRuO_3$. Furthermore, the peak in the $SrCo_{0.5}Ru_{0.5}O_{2.96}$ spectrum is observed at ~1.35 eV higher in energy than that of the Ru^{4+} reference $SrRuO_3$. The upward chemical shift from $SrRuO_3$ to $SrCo_{0.5}Ru_{0.5}O_{2.96}$ reflects the increase in the ruthenium valence from Ru^{4+} to Ru^{5+}.[33] In order to understand the different spectral features and further confirm the Ru^{5+} state in $SrCo_{0.5}Ru_{0.5}O_{2.96}$, simulations of the Ru-$L_{2,3}$ XAS spectra were carried out for the Ru^{4+} and Ru^{5+} states using

dx.doi.org/10.1021/ja4114006 | J. Am. Chem. Soc. 2014, 136, 1514−1519

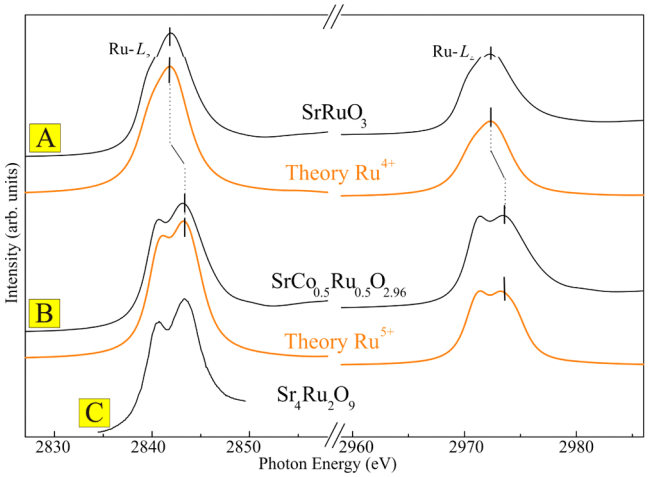

Figure 3. Room-temperature (black lines) Ru-$L_{2,3}$ XAS spectra of (A) $SrRuO_3$, (B) $SrCo_{0.5}Ru_{0.5}O_{2.96}$, and (C) $Sr_4Ru_2O_9$.[33] Simulations (red lines) for a Ru^{5+} and Ru^{4+} ion in octahedral coordination are also plotted below the experimental data.

multiplet calculations, in which the effects of hybridization were taken into account i.e. a configuration interaction cluster model.[34] Using a set of physically reasonable parameters,[35] the theoretical simulations reproduce excellently the experimental results of both $SrRuO_3$ and $SrCo_{0.5}Ru_{0.5}O_{2.96}$ as shown in Figure 3. Hence, ruthenium is found to be 5+ in the title compound.

Having established the Ru^{5+} state in $SrCo_{0.5}Ru_{0.5}O_{2.96}$, the Co^{3+} state is now required for charge balance. To confirm this, the Co-$L_{2,3}$ XAS spectra were measured (Figure 4B) and compared with those of $BaCoO_3$ (Figure 4A) as a Co^{4+} reference,[36] $LaCoO_3$ at 20 and 650 K as a Co^{3+} species (Figure 4C),[10] and CoO as a compound with Co^{2+} (Figure 4D). The spectral weight of the L_3 white line shifts to higher energies as

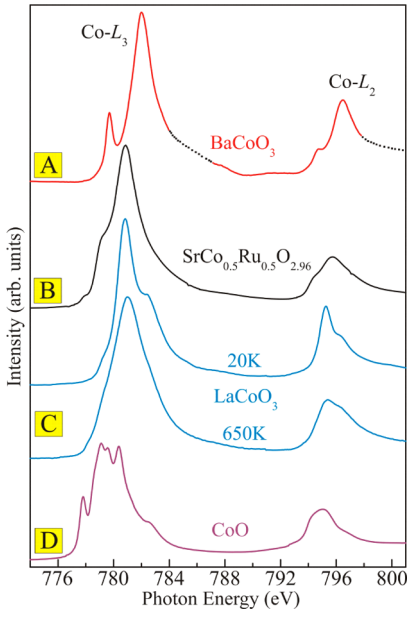

Figure 4. Experimental Co-$L_{2,3}$ XAS spectra of (A) $BaCoO_3$ taken from Lin et al.,[36] (B) $SrCo_{0.5}Ru_{0.5}O_{2.96}$, (C) $LaCoO_3$ at 20 and 650 K taken from Haverkort et al.[10] and (D) CoO. The data are recorded at room-temperature unless stated specifically in the figure.

the cobalt oxidation state increases: from Co^{2+} (CoO) through Co^{3+} ($LaCoO_3$) to Co^{4+} ($BaCoO_3$). This reflects that X-ray absorption spectra at the transition-metal $L_{2,3}$ edge are highly sensitive to the valence state.[31,36−38] Obviously, the spectrum of the title compound (Figure 4B) shows the closest resemblance (but is not identical) to that of $LaCoO_3$ at 650 K (Figure 4C), indicating a Co^{3+} valence state. Thus, all XAS measurements safely rule out the Co^{4+}/Ru^{4+} scenario.[26]

The spin state of cobalt. While there is little doubt about the $S = 3/2$ spin state of the Ru^{5+} ($4d^3$) ion, the spin state of the Co^{3+} ion in title compound needs to be identified. In Figure 5A

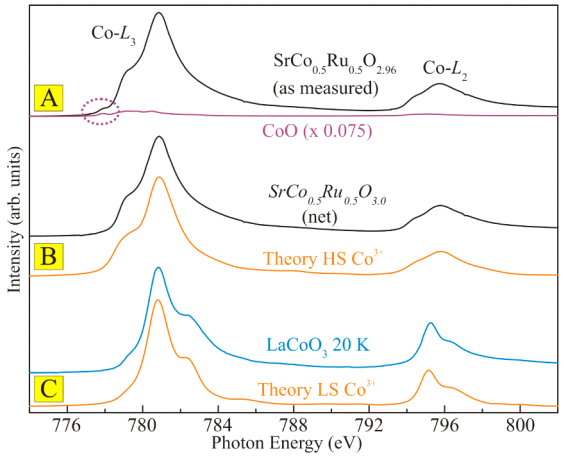

Figure 5. (A) Co-$L_{2,3}$ XAS spectra of $SrCo_{0.5}Ru_{0.5}O_{2.96}$ and CoO, (B) net $SrCo_{0.5}Ru_{0.5}O_{3.0}$ ($SrCo_{0.5}Ru_{0.5}O_{2.96}$ minus 7.5% CoO), (C) $LaCoO_3$ at 20 K. Theoretical Co-$L_{2,3}$ XAS spectra of HS and LS Co^{3+} are plotted next to their expected equivalent. All data are obtained at room-temperature and a dashed circle marks the Co^{2+} prepeak.

the Co-$L_{2,3}$ XAS spectrum is shown again. Here we notice a minor prepeak at 778 eV, which can be attributed to the presence of a Co^{2+} species. From our thermal reduction experiment (S1 in SI), we found that the material is slightly oxygen deficient (2.96 instead of 3.00), so that we indeed can expect the presence of some small amount of Co^{2+}. By subtracting a 7.5% Co^{2+} spectrum from the as-measured title compound we obtain an XAS-$L_{2,3}$ spectrum, which is free from any features in this prepeak region (Figure 5B). This spectrum can now be quantitatively analyzed by using well proven configuration interaction cluster model that include the full multiplet theory.[10,34] Using this cluster model analysis, the LS Co^{3+} of $LaCoO_3$ at 20 K[10] is readily reproduced, and the simulation excellently agrees with the nonmagnetic ground state of $LaCoO_3$ (Figure 5C). By applying the same set of parameters[39] and changing only the Co 3d − O 2p hybridization strength according to Harrison,[40] a remarkable agreement between experimental data and simulated spectrum is obtained (Figure 5B). The increase in average Co−O bond length, namely 1.925 Å in $LaCoO_3$ at 20 K[41] to 1.98(2) Å in $SrCo_{0.5}Ru_{0.5}O_{2.96}$ causes the drastic change in hybridization and crystal field strength. Now, the simulated spectrum corresponds to an octahedrally coordinated Co^{3+} ion in the HS state instead. This proves the HS ground state of the Co ions in the title compound. Note that the $L_{2,3}$ XAS spectrum for a HS ion is clearly different from that of a LS ion, confirming the high sensitivity of soft XAS as reported earlier.[42] We would also like to add that the excellent agreement between the experimental

dx.doi.org/10.1021/ja4114006 | J. Am. Chem. Soc. 2014, 136, 1514−1519

and simulated XAS spectra, including the fine details in the atomic-like multiplet features, can be taken as an *a posteriori* justification to analyze the magnetic properties of the system starting from the local electronic properties of the ions involved.

Pressure-Dependent Spin State Transition of Cobalt. To investigate whether the HS state in $SrCo_{0.5}Ru_{0.5}O_{2.96}$ can be converted to an IS or LS state on applying pressure, a Kβ emission experiment[18,43−46] was carried out. Figure 6A shows

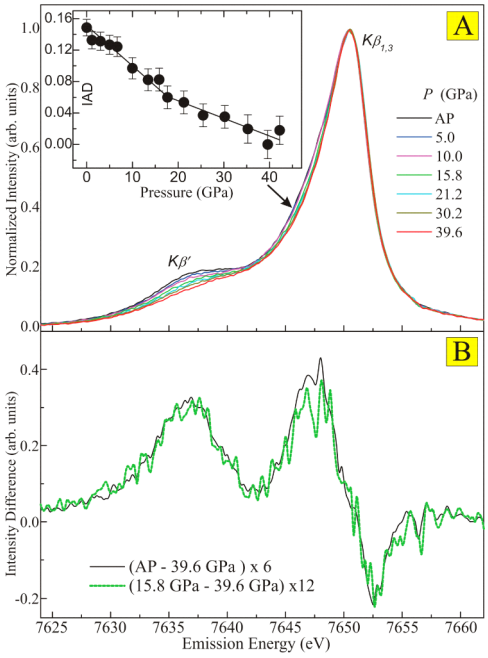

Figure 6. (A) Evolution of the Co Kβ X-ray emission spectra of $SrCo_{0.5}Ru_{0.5}O_{2.96}$ under pressure up to 39.6 GPa at room-temperature. (Inset) IAD values of Co Kβ emission spectra as a function of applied pressure with respect to 39.6 GPa. (B) Difference spectra of Co Kβ emissions taken at ambient pressure (AP) and 39.6 GPa (full black line) and at 15.8 and 39.6 GPa (green dashed line).

the evolution of the Co Kβ X-ray emission line of the title compound as a function of pressure from ambient up to 39.6 GPa at room temperature. At ambient pressure, the Co Kβ emission spectrum reveals a main peak located at ~7650 eV referred to as the K$\beta_{1,3}$ line and a pronounced satellite peak located at ~7637 eV corresponding to the Kβ' line. This line-shape defines the Kβ emission spectrum for a HS Co^{3+}. At high pressures, e.g. 39.6 GPa, the satellite peak nearly disappear, and the main line gets narrower. This is similar to what happens for the Kβ emission spectrum of $LaCoO_3$ at low temperatures,[45] indicating that the LS state has been reached for $SrCo_{0.5}Ru_{0.5}O_{2.96}$. In fact, the spectral changes are alike those found for the complete spin state transition in FeS from 0 to 11.5 GPa[43] and for $Mg_{0.9}Fe_{0.1}SiO_3$[44] from 20 to 120 GPa, where Fe^{2+} also has the $3d^6$ electronic configuration. This infers that the applied pressure induces a complete HS to LS transition in the title compound.

The intensity of the Kβ' satellite peak is widely applied to estimate the local 3d spin moment of transition metal ions.[18,45−47] The inset of Figure 6A contains a plot of the so-called integrated absolute difference (IAD)[18,45−47] as a function of pressure, and the total IAD changes by about 0.15 in going from ambient pressure to 39.6 GPa. This 0.15 value is consistent with what is expected for a complete HS to LS transition. We note that the Kβ emission experiment is not sensitive enough to detect separately the presence of the high-spin Co^{2+} impurities nor the possible presence of Co^{3+} ions with finite spin states[48] associated with the oxygen defects in the few percent range ($SrCo_{0.5}Ru_{0.5}O_{3-\delta}$ with δ = 0.04).

It is important that the spectral changes with pressure are continuous without any signs for new features that otherwise could indicate the presence of spin states other than the HS and LS. This is apparent in Figure 6B, displaying a comparison between the difference spectrum of Kβ emissions taken at ambient pressure (AP) and 39.6 GPa (black line) with the difference spectrum of emissions obtained at 15.8 and 39.6 GPa (green line). The black curve represents the spectral changes associated with a change in the average spin expectation value $\overline{S}$ from 2 to 0, and the green curve for a change of $\overline{S}$ from ~1 to 0. Note that the difference spectra are identical apart from the expected scaling factor of 2. This means that the system at 15.8 GPa is in a ~1:1 mixed HS:LS state, and not in an IS state, as otherwise the difference spectrum would show new features.[45]

Stability of the Ruthenium Oxidation State. Perhaps it is a bit superfluous, but we also would like to make sure that the reduction of spin moment of the cobalt ions under pressure is not caused by a change of the Co configuration from HS Co^{3+} (S = 2) to LS Co^{4+} (S = 1/2) accompanied with a change of the Ru valence from 5+ to 4+. For this purpose the Ru−K XAS spectra were obtained under pressures up to 30.5 GPa. As shown in Figure 7, there is no energy shift at the Ru-K edge

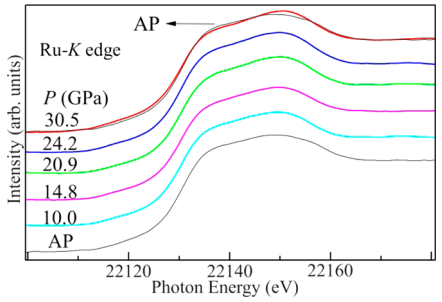

Figure 7. Pressure dependence of the Ru−K XAS spectra of $SrCo_{0.5}Ru_{0.5}O_{2.96}$ at room-temperature. The data at ambient pressure (AP) and at 30.5 GPa are superpositioned (top) to emphasize the negligible pressure dependence of the Ru−K spectrum.

with pressure, indicating the ruthenium valence remains 5+. Thus, this reaffirms that the decrease of the cobalt moment under pressure is solely due to a gradual spin state transition of Co^{3+} ions without involving any valence state changes of the cobalt ions.

Crystal Field Effects on the Cobalt spin state. To understand the above experimental observations, the total energy level diagram of the cobalt ions as a function of Co−O distance was calculated (Figure 8). Clearly, the ground state of Co^{3+} ions is either HS or LS (not IS) with a crossover at Co−O distance about 1.93 Å, where the HS and LS states are strongly mixed or, when local lattice relaxations are allowed to take place,[10] coexist incoherently on different (and possibly neighboring) sites, as speculated earlier by Raccah and Goodenough for the high temperature phase of $LaCoO_3$.[9] Thus, Figure 8 describes the evolution of the spin state during the compression induced by high pressure for $SrCo_{0.5}Ru_{0.5}O_{2.96}$

dx.doi.org/10.1021/ja4114006 | J. Am. Chem. Soc. 2014, 136, 1514−1519

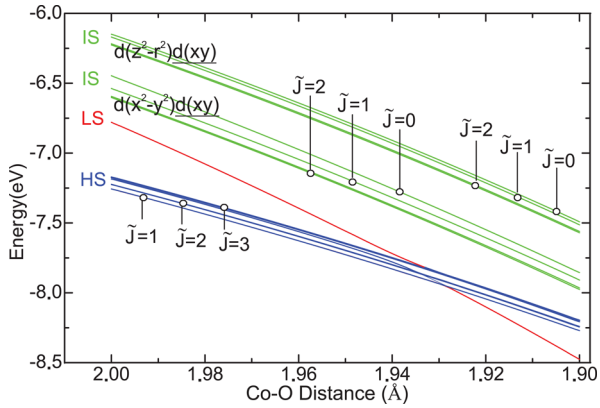

Figure 8. Energy level diagram of a CoO_6 cluster as a function of the Co−O distance.

and, conversely, during the expansion upon increasing the temperature for $LaCoO_3$.

Note that the IS states are remarkably unfavorable in energy in comparison to the HS and LS states. In fact, the lowest of the IS states is already ∼0.4 eV (∼4000 K) higher than the degenerated LS and HS at the Co−O distance 1.932 Å. It is not clear whether a Jahn−Teller distortion could stabilize the IS states.[49] Simulations by Haverkort[50] show that the lowest IS states are not Jahn−Teller active: they are of the $d(x^2-y^2)\underline{d(xy)}$ type,[51] so the e_g electron (x^2-y^2) and the t_{2g} hole lie in the same $x-y$ plane. The Jahn−Teller active IS states are of the type $d(3z^2-r^2)\underline{d(xy)}$, but these are even higher in energy by ∼0.8 eV (∼8000 K), so that extremely large distortions are needed to stabilize them relative to the HS or LS states. Hence, it is concluded from these local electronic and atomic considerations that very special crystal structures are obligatory to stabilize an IS state (if at all) for insulating Co^{3+} oxides. We would like to note that for metallic cobaltates, in which inter-Co charge fluctuations play an important role, the concept of local spin states may no longer be meaningful and that the discussion of the magnetic properties of such systems may need a more complicated (and probably presently unsolvable) theoretical model where the wave-vector dependence of the self-energy $\sum(k,\omega)$ is also taken into account.

4. CONCLUSIONS

We have discovered that the Co^{3+} ion in $SrCo_{0.5}Ru_{0.5}O_{2.96}$ is high-spin, which is unique for Co^{3+} in octahedral oxygen coordination. Further, we have shown that it was possible to induce a complete spin state transition using high pressure. All pressure-dependent data can be understood by a gradual change from a high-spin state at ambient pressure to a low-spin state at about 40 GPa. As Ru^{5+} is unaffected by pressure, the spin state transition of Co^{3+} solely is responsible for the change in magnetic moment. We have not found any signs of the much debated intermediate spin state at any stage during the pressure induced spin state transition. Model calculations provide a quantitative estimate for the relative stability of the high-, intermediate-, and low-spin states as functions of the metal−oxygen bond length for a Co^{3+} ion in an octahedral coordination.

■ ASSOCIATED CONTENT

Supporting Information

Thermogravimetric data including the reduction conditions and evaluation of the data; X-ray diffraction experiment and the Rietveld fit to the observed data. This material is available free of charge via the Internet at http://pubs.acs.org.

■ AUTHOR INFORMATION

Corresponding Author

martin.valldor@cpfs.mpg.de

Notes

The authors declare no competing financial interest.

■ ACKNOWLEDGMENTS

This research was supported by the NSRRC and the National Science Council of Republic of China (Grant NSC 102-2113-M-213-004-MY3) and by the German Science Foundation (DFG) through SFB608. Y.Y. Chin received financial support from the European Union through the ITN Soprano Network.

■ REFERENCES

(1) Stoufer, R. C.; Busch, D. H.; Hadley, W. B. *J. Am. Chem. Soc.* **1961**, *83*, 3732−3734.
(2) Jenkins, D. M.; Peters, J. C. *J. Am. Chem. Soc.* **2003**, *125*, 11162−11163.
(3) Krivokapic, I.; Zerara, M.; Lawson Dakua, M.; Vargas, A.; Enachescu, C.; Ambrus, Ch.; Tregenna-Piggott, P.; Amstutz, N.; Krausz, E.; Hauser, A. *Coord. Chem. Rev.* **2007**, *251*, 364−378.
(4) Hanawa, H.; Moritomo, Y.; Tateishi, J.; Ohishi, Y.; Kato, K. *J. Phys. Soc. Jpn.* **2004**, *73*, 2759−2762.
(5) Cowan, M. G.; Olguín, J.; Narayanaswamy, S.; Tallon, J. L.; Brooker, S. *J. Am. Chem. Soc.* **2012**, *134*, 2892−2894.
(6) Suresh, N.; Cowan, M. G.; Olguin, J.; Tallon, J. L.; Brooker, S. *Proc. 36th Ann. Cond. Matter Mater.* **2012**, FO 06.
(7) Oku, M. *J. Solid State Chem.* **1978**, *23*, 177−185.
(8) Hu, Z.; Mazumdar, C.; Kaindl, G.; de Groot, F. M. F.; Warda, S. A.; Reinen, D. *Chem. Phys. Lett.* **1998**, *297*, 321−328.
(9) Goodenough, J. B.; Raccah, P. M. *J. Appl. Phys.* **1965**, *36*, 1031−1032.
(10) Haverkort, M. W.; Hu, Z.; Cezar, J. C.; Burnus, T.; Hartmann, H.; Reuther, M.; Zobel, C.; Lorenz, T.; Tanaka, A.; Brookes, N. B.; Hsieh, H. H.; Lin, H. -J.; Chen, C. T.; Tjeng, L. H. *Phys. Rev. Lett.* **2006**, *97*, 176405.
(11) Yamaura, K.; Zandbergen, H. W.; Abe, K.; Cava, R. J. *J. Solid State Chem.* **1999**, *146*, 96−102.
(12) Matsuno, J.; Okimoto, Y.; Fang, Z.; Yu, X. Z.; Matsui, Y.; Nagaosa, N.; Kawasaki, M.; Tokura, Y. *Phys. Rev. Lett.* **2004**, *93*, 167202.
(13) Potze, R. H.; Sawatzky, G. A.; Abbate, M. *Phys. Rev. B* **1995**, *51*, 11501−11506.
(14) Jin, R.; Sha, H.; Khalifah, P. G.; Sykora, R. E.; Sales, B. C.; Mandrus, D.; Zhang, J. *Phys. Rev. B* **2006**, *73*, 174404.
(15) Hollmann, N.; Hu, Z.; Valldor, M.; Maignan, A.; Tanaka, A.; Hsieh, H. H.; Lin, H. -J.; Chen, C. T.; Tjeng, L. H. *Phys. Rev. B* **2009**, *80*, 085111.
(16) Hu, Z.; Wu, H.; Haverkort, M. W.; Hsieh, H. H.; Lin, H. -J.; Lorenz, T.; Baier, J.; Reichl, A.; Bonn, I.; Felser, C.; Tanaka, A.; Chen, C. T.; Tjeng, L. H. *Phys. Rev. Lett.* **2004**, *92*, 207402.
(17) Belik, A. A.; Iikubo, S.; Kodama, K.; Igawa, N.; Shamoto, S.; Niitaka, S.; Azuma, M.; Shimakawa, Y.; Takano, M.; Izumi, F.; Takayama-Muromachi, E. *Chem. Mater.* **2006**, *18*, 798−803.
(18) Oka, K.; Azuma, M.; Chen, W.; Yusa, H.; Belik, A. A.; Takayama-Muromachi, E.; Mizumaki, M.; Ishimatsu, N.; Hiraoka, N.; Tsujimoto, M.; Tucker, M. G.; Attfield, J. P.; Shimakawa, Y. *J. Am. Chem. Soc.* **2010**, *132*, 9438−9443.
(19) Kanungo, S.; Saha Dasgupta, T. *Phys. Rev. B* **2011**, *83*, 104104.

(20) Martin, C.; Maignan, A.; Pelloquin, D.; Nguyen, N.; Raveau, B. *Appl. Phys. Lett.* **1997**, *71*, 1421−1423.
(21) Kobayashi, W.; Ishiwata, S. *Phys. Rev. B* **2005**, *72*, 104408.
(22) Tsubouchi, S.; Kyômen, T.; Itoh, M.; Ganguly, P.; Oguni, M.; Shimojo, Y.; Morii, Y.; Ishii, Y. *Phys. Rev. B* **2002**, *66*, 052418.
(23) Knížek, K.; Jirák, Z.; Hejtmánek, J.; Novák, P.; Ku, W. *Phys. Rev. B* **2009**, *79*, 014430.
(24) Hsu, H.; Blaha, P.; Wentzcovitch, R. M.; Leighton, C. *Phys. Rev. B* **2010**, *82*, 100406.
(25) Kim, S. H.; Battle, P. D. *J. Solid State Chem.* **1995**, *114*, 174−183.
(26) Lozano-Gorrin, A. D.; Greedan, J. E.; Núñez, P.; González-Silgo, C.; Botton, G. A.; Radtke, G. *J. Solid State Chem.* **2007**, *180*, 1209−1217.
(27) Takada, K.; Sakurai, H.; Takayama-Muromachi, E.; Izumi, F.; Dilanian, R. A.; Sasaki, T. *Nature (London)* **2003**, *422*, 53−55.
(28) Pérez, J.; García, J.; Blasco, J.; Stankiewicz, J. *Phys. Rev. Lett.* **1998**, *80*, 2401−2404.
(29) Terasaki, I.; Sasago, Y.; Uchinokura, K. *Phys. Rev. B* **1997**, *56*, R12685−R12687.
(30) Maignan, A.; Caignaert, V.; Raveau, B.; Khomskii, D.; Sawatzky, G. *Phys. Rev. Lett.* **2004**, *93*, 026401.
(31) Chang, C. F.; Hu, Z.; Wu, H.; Burnus, T.; Hollmann, N.; Benomar, M.; Lorenz, T.; Tanaka, A.; Lin, H. -J.; Hsieh, H. H.; Chen, C. T.; Tjeng, L. H. *Phys. Rev. Lett.* **2009**, *102*, 116401.
(32) Asai, K.; Yoneda, A.; Yokokura, O.; Tranquada, J. M.; Shirane, G.; Kohn, K. *J. Phys. Soc. Jpn.* **1998**, *67*, 290−296.
(33) Hu, Z.; Golden, M. S.; Ebbinghaus, S. G.; Knupfer, M.; Fink, J.; de Groot, F. M. F.; Kaindl, G. *Chem. Phys.* **2002**, *282*, 451−463.
(34) Tanaka, A.; Jo, T. *J. Phys. Soc. Jpn.* **1994**, *63*, 2788−2807.
(35) RuO_6 cluster parameters (eV): U_{dd} = 3.0, Slater integrals 70% of Hartree−Fock values. Δ = 2.0 and −1. 10Dq = 1.3 and 2.15, and $pd\sigma$ = −2.52 and −2.78 for Ru^{4+} and Ru^{5+}, respectively.
(36) Lin, H. -J.; Chin, Y. Y.; Hu, Z.; Shu, G. J.; Chou, F. C.; Ohta, H.; Yoshimura, K.; Hebert, S.; Maignan, A.; Tanaka, A.; Tjeng, L. H.; Chen, C. T. *Phys. Rev. B* **2010**, *81*, 115138.
(37) Burnus, T.; Hu, Z.; Hsieh, H. H.; Joly, V. L. J.; Joy, P. A.; Haverkort, M. W.; Wu, H.; Tanaka, A.; Lin, H. -J.; Chen, C. T.; Tjeng, L. H. *Phys. Rev. B* **2006**, *74*, 245111.
(38) Burnus, T.; Hu, Z.; Hsieh, H. H.; Joly, V. L. J.; Joy, P. A.; Haverkort, M. W.; Wu, H.; Tanaka, A.; Lin, H. -J.; Chen, C. T.; Tjeng, L. H. *Phys. Rev. B* **2008**, *77*, 125124.
(39) Cluster CoO_6 parameters (eV): U_{dd} = 5.5, Δ = 2.0, Slater integrals 80% of Hartree−Fock values. 10Dq = 0.5 and 0.6, and $pd\sigma$ = −1.54 and −1.70 for $SrCo_{0.5}Ru_{0.5}O_3$ and $LaCoO_3$, respectively.
(40) Harrison, W. A. *Electronic Structure and the Properties of Solids*; Dover: New York, 1989.
(41) Radaelli, P. G.; Cheong, S.-W. *Phys. Rev. B* **2002**, *66*, 094408.
(42) Cartier dit Moulin, C.; Rudolf, P.; Flank, A. M.; Chen, C. T. *J. Phys. Chem.* **1992**, *96*, 6196−6198.
(43) Rueff, J. -P.; Kao, C.-C.; Struzhkin, V. V.; Badro, J.; Shu, J.; Hemley, R. J.; Mao, H. K. *Phys. Rev. Lett.* **1999**, *82*, 3284−3287.
(44) Badro, J.; Rueff, J.-P.; Vankó, G.; Monaco, G.; Fiquet, G.; Guyot, F. *Science* **2004**, *305*, 383−386.
(45) Vankó, G.; Rueff, J.-P.; Mattila, A.; Németh, Z.; Shukla, A. *Phys. Rev. B* **2006**, *73*, 024424.
(46) Lengsdorf, R.; Rueff, J.-P.; Vankó, G.; Lorenz, T.; Tjeng, L. H.; Abd-Elmeguid, M. M. *Phys. Rev. B* **2007**, *75*, 180401.
(47) Mattila, A.; Pylkkänen, T.; Rueff, J.-P.; Huotari, S.; Vankó, G.; Hanfland, M.; Lehtinen, M.; Hämäläinen, K. *J. Phys.: Condens. Matter* **2007**, *19*, 386206.
(48) He, C.; Zheng, H.; Mitchell, J. F.; Foo, M. L.; Cava, R. J.; Leighton, C. *Appl. Phys. Lett.* **2009**, *94*, 102514.
(49) Maris, G.; Ren, Y.; Volotchaev, V.; Zobel, C.; Lorenz, T.; Palstra, T. T. M. *Phys. Rev. B* **2003**, *67*, 224423.
(50) Haverkort, M. W. *Spin and Orbital Degrees of Freedom in Transition Metal Oxides and Oxide Thin Films Studied by Soft X-ray Absorption Spectroscopy*. PhD Thesis 2005, p 127, University of Cologne; http://kups.ub.unikoeln.de/1455/
(51) Korotin, M. A.; Ezhov, S. Y.; Solovyev, I. V.; Anisimov, V. I.; Khomskii, D. I.; Sawatzky, G. A. *Phys. Rev. B* **1996**, *54*, 5309−5316.